Inequivalence of the Two Tyrosine Ligands in the N-Lobe of Human Serum Transferrin†

Qing-Yu He,*,‡ Anne B. Mason,‡ Robert C. Woodworth,‡ Beatrice M. Tam,§ Ross T. A. MacGillivray,§ John K. Grady,|| and N. Dennis Chasteen||

Department of Biochemistry, College of Medicine, University of Vermont, Burlington, Vermont 05405, Department of Biochemistry and Molecular Biology, University of British Columbia, Vancouver, BC V6T 1Z3, Canada, and Department of Chemistry, Parsons Hall, University of New Hampshire, Durham, New Hampshire 03824

Received August 8, 1997; Revised Manuscript Received September 22, 1997⊗

ABSTRACT: Human serum transferrin N-lobe (hTF/2N) has four iron-binding ligands, including one histidine, one aspartate, and two tyrosines. The present report elucidates the inequivalence of the two tyrosine ligands (Tyr 95 and Tyr 188) on the metal-binding properties of hTF/2N by means of site-directed mutagenesis, metal release kinetics, and absorption and electron paramagnetic resonance (EPR) spectroscopies. When the liganding tyrosines were mutated individually to phenylalanine, the resulting mutant Y95F showed a weak binding affinity for iron and no affinity for copper, whereas, mutant Y188F completely lost the ability to bind iron but formed a stable complex with copper. Since other studies have demonstrated that mutations of the other two ligands, histidine and aspartate, did not completely abolish iron binding, the present findings suggest that the tyrosine ligand at position 188 is essential for binding of iron to occur. Replacement of Tyr 188 with phenylalanine created a favorable chemical environment for copper coordination but a fatal situation for iron binding. The positions of the two liganding tyrosines in the metal-binding cleft suggest a reason for the inequivalence.

Human serum transferrin (hTF)[1] is a member of the transferrin family of iron-binding proteins. It reversibly binds iron in blood plasma and transports iron to cells requiring iron (*1*−*3*). The full-length transferrin molecule (∼80 kDa) has two similar halves, the N-lobe and C-lobe, linked by a short bridging peptide. Each lobe carries an iron-binding site, surrounded by two dissimilar domains (NI and NII domains for N-lobe and CI and CII domains for C-lobe) which make up the binding cleft. When iron is released, the two domains within each lobe rotate around two hinges to form an "open" conformation (*4*). Crystallographic studies of four homologous proteins, human lactoferrin (hLF) (*5*), human serum transferrin (hTF) (*6*), rabbit serum transferrin (rTF) (*7*), and chicken ovotransferrin (oTF) (*8*), have shown that the iron coordination in the binding sites is the same, with the ferric ion bound octahedrally to four protein ligands (two tyrosines, one aspartate, and one histidine) and two oxygens from the synergistic anion, carbonate. In the sequence of the N-lobe in human serum transferrin (hTF/2N), the ligands are Tyr 95, Tyr 188, Asp 63, and His 249, with Asp 63 on the NI domain, Tyr 188 on the NII domain, and Tyr 95 and His 249 on the hinge strands (Figure 1). Besides binding iron, transferrin can bind other di-, tri-, and tetravalent metal ions (*9*−*14*). Other anions possessing a carboxylate group are also able to serve as the "synergistic anion", coordinating to the metal center in the place of carbonate (*15*, *16*). Numerous studies involving the binding of transferrins with various metal ions and anions have been conducted to help understand the biophysical properties of these proteins (*16*−*20*).

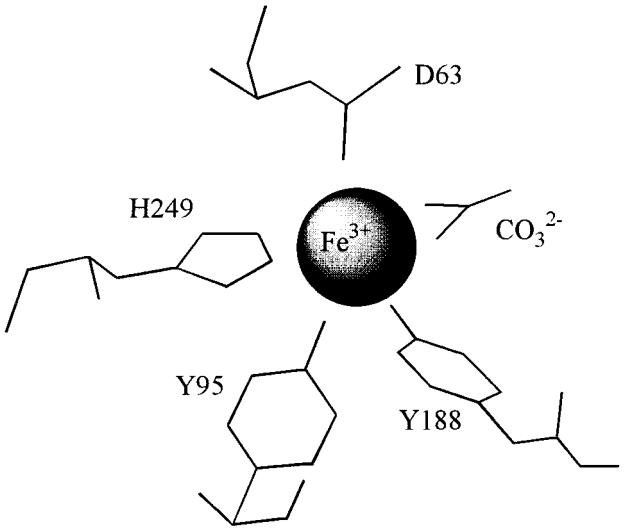

FIGURE 1: A schematic diagram showing the metal binding site in the N-lobe of human serum transferrin.

Recombinant DNA techniques have been used to explore the specific role a binding ligand plays in the metal-binding

†This work was supported by USPHS Grant R01 DK 21739 (to R.C.W.) from the National Institute of Diabetes, and Digestive and Kidney Diseases and Grant R37 GM 20194 (to N.D.C.) from the National Institute of General Medical Sciences. Q.-Y.H. was supported by the Dean's Postdoctoral Fellowship from the College of Medicine at the University of Vermont.

* Corresponding author. Telephone: (802) 656-0343. Fax: (802) 862-8229. E-mail: qhe@zoo.uvm.edu.

‡ University of Vermont.

§ University of British Columbia.

|| University of New Hampshire.

⊗ Abstract published in *Advance ACS Abstracts,* November 15, 1997.

[1] Abbreviations: hTF, human serum transferrin; hTF/2N, recombinant N-lobe of human transferrin comprising residues 1−337; mutants of hTF/2N are designated by the wild type amino acid residue, the sequence number and the amino acid to which the residue was mutated; BHK, baby hamster kidney cells; NTA, nitrilotriacetate; EDTA, ethylenediaminetetraacetate; EDDA, ethylenediamine-*N*,*N*′-diacetate; Tiron, 4,5-dihydroxy-1,3-benzenedisulfonate; EPR, electron paramagnetic resonance.

S0006-2960(97)01955-7 CCC: $14.00

properties of transferrin. Mutants of the histidine ligand and the aspartate ligand in the N-lobe of both lactoferrin (*21*, *22*) and human serum transferrin (*23*−*26*) have been prepared and characterized. Not surprisingly, structural and metal-binding studies have demonstrated that mutations of these ligands substantially alter the coordination and metal-binding properties of the proteins (*21*, *22*). These mutants generally do not lose their iron-binding ability completely even when the liganding residue is changed to a noncoordinating residue such as alanine or phenylalanine (*22*, *26*). Previous studies with lactoferrin showed that when the two liganding tyrosines in a lobe were both mutated to alanine, the resulting mutants failed to bind iron (*27*). Mutant Y95H of hTF/2N released iron similarly to the parent hTF/2N protein (*25*). However, the specific effects from individual tyrosine ligands on the functions of transferrin have not been previously investigated in detail. In the present report, three single-point tyrosine mutants of hTF/2N (Y95F, Y96F, and Y188F) have been produced, purified, and characterized. In the cases of mutants Y95F and Y188F, where the metal coordination of the tyrosine side chain was disabled, the importance of each tyrosine ligand has been addressed by a number of different techniques including high-resolution EPR. The results show that the two tyrosine ligands are inequivalent in their effect on the metal-binding properties of transferrin. Tyrosine 188 is the most critical ligand for natural iron-binding; without it, the iron binding ability of N-lobe transferrin is entirely abolished.

MATERIALS AND METHODS

Materials. Chemicals were reagent grade. Stock solutions of HEPES, MES, and other buffers were prepared by dissolving the anhydrous salts in Milli-Q (Millipore) purified water and adjusting the pH to desired values with 1 N NaOH or HCl. Standard solutions of copper(II) (10 000 μg/mL) and iron(II) (1000 μg/mL) in 5% HNO_3 were obtained from Johnson Matthey. 4,5-Dihydroxy-1,3-benzenedisulfonate (Tiron) came from Fisher Scientific Co., ethylenediaminetetraacetate (EDTA) from Mann Research Laboratories, Inc., ethylenediamine-*N*,*N*′-diacetate (EDDA) from Aldrich Chemical Co., and nitrilotriacetate (NTA) from Sigma. Centricon 10 microconcentrators were from Amicon.

DNA Manipulations. Mutations Y95F, Y96F, and Y188F were constructed by using a polymerase chain reaction (PCR) based mutagenesis procedure (*28*). The following oligonucleotides were used for the mutagenesis experiments:

Y95F: 5′-CAGACTTTCTTTTATGCTGTT-3′

Y96F: 5′-ACTTTCTATTTTGCTGTTGCT-3′

Y188F: 5′-TACTTCGGCTTCTCGGGAGCC-3′

To obtain a template for the PCR-based mutagenesis, the plasmid BS hTF/2N (*29*), containing DNA coding for the N-lobe of transferrin as an *Xba*I−*Hind*III fragment cloned into Bluescript, was cleaved with *Bam*HI and *Eco*RI, and the resulting DNA fragment (containing nucleotides 354−928 of the cDNA) was isolated by gel electrophoresis. This DNA fragment was cloned into the *Bam*HI and *Eco*RI sites of Bluescript, and used as a template for each of the three mutagenesis reactions using the appropriate mutagenic oligonucleotide and following a protocol similar to that already described in detail (*26*). The complete nucleotide sequences of the cloned fragments were then determined to confirm the presence of the desired mutation and the absence of PCR-induced mutations. The Bluescript hTF/2N constructs containing the point mutations were then cleaved with *Xba*I and *Hind*III to release the DNA coding for the N-lobe and inserted into the *Sma*I site of pNUT as described (*26*).

Expression, Purification, and Preparation of Proteins. The N-lobe of hTF and the single point tyrosine mutants of hTF/2N were expressed into the medium of baby hamster kidney (BHK) cells containing the relevant cDNA in the pNUT vector and were purified as reported previously (*23*, *30*). The preparation of apo- and Fe-loaded protein samples followed the procedure described previously (*26*). To prevent the possibility of NTA taking part in the ligation in the metal binding of the proteins, as was found with the aspartate mutants (*26*), iron(II)-nitrate instead of ferric NTA was used to load the tyrosine mutants in the presence of bicarbonate (25 mM). Substantial time (2 h at room temperature or overnight in 4 °C) is required for equilibrium (conversion of the ferrous form of iron to the ferric form) and formation of the natural complex of hTF/2N with the synergistic carbonate anion. A slight excess of copper(II)-nitrate was used to prepare the Cu-saturated transferrin.

To make the ^{63}Cu protein samples, a 20 mM $^{63}Cu(NO_3)_2$ solution was first prepared by dissolving 7 mg of ^{63}Cu metal (Cambridge Isotopes) in 0.5 mL of 6 N HNO_3 for 3 h, followed by evaporation to dryness under a stream of dry N_2. The copper nitrate was then dissolved and brought to volume with 0.01 N DCl. ^{63}Cu-transferrin samples were then prepared by dissolving the lyophilized apoprotein in 99.9% D_2O containing 100 mM HEPES and 20 mM $NaHCO_3$, pD = 7.9 adjusted with 40% NaOD and 20% DCl (pD = pH meter reading + 0.40, calibrated with standard H_2O buffers) followed by addition of $^{63}Cu(NO_3)_2$ solution to 90% saturate the 0.50 mM protein. After incubation for 3 h at room temperature, the samples were then frozen in 3.0 mm i.d. − 4.0 mm o.d. quartz tubes for EPR measurement.

Spectra and Metal-Binding Titration. UV−vis spectra were recorded on a Cary 219 spectrophotometer under the control of the computer program Olis-219s (On-line Instrument Systems, Inc., Bogart, GA). The appropriate buffer served as the reference for full-range spectra from 236 to 650 nm. Difference spectra were generated by storing the spectrum of the apo-protein as the baseline and subtracting it from the sample spectra. This results in small differences in the absorption maxima when compared to the normal spectrum. Co(III) titrations were carried out as described previously (*19*). Titration with Cu(II) and Fe(II) followed a similar protocol. Titration of wild-type hTF/2N was performed prior to titration of each mutant sample to standardize the procedure. The reported results are the average values derived from at least two titrations.

Kinetics of Metal Release. As described in detail (*26*), kinetics of metal removal from transferrin were measured by monitoring the change of UV−visible absorbance at 480 nm (for the iron release with Tiron) or at the λ_{max}s (Table 1) (for the metal removal with EDDA and EDTA). The absorbance *vs* time data were recorded until at least three half-lives had elapsed. Tiron and EDDA were used as chelators for iron release and EDTA was used as a chelator for copper removal. All data were analyzed with single-

Table 1: Summary of the Spectral Characteristics and Extinction Coefficients for Recombinant Wild-Type (WT) and Mutants of hTF/2N

	Fe-hTF/2N-CO_3 complex				Cu-hTF/2N-CO_3 complex				Apo-hTF/*2N*
protein	λ_{max} (nm)	λ_{min} (nm)	A_{max}/A_{min}	A_{280}/A_{max}	λ_{max} (nm)	λ_{min} (nm)	A_{max}/A_{min}	A_{280}/A_{max}	ϵ_{280} (mM^{-1} cm^{-1})
Y95F	410	390	1.02 ± 0.01	44.4 ± 0.4					36.87[a]
Y96F	475	410	1.38 ± 0.01	23.3 ± 0.2	425	365	1.83 ± 0.01	30.9 ± 0.1	38.4 ± 0.2[b]
Y188F					420	365	1.90 ± 0.01	28.5 ± 0.3	37.2 ± 0.2[c]
WT	472	410	1.37 ± 0.02	23.5 ± 0.1	425	365	1.82 ± 0.01	31.1 ± 0.2	38.5 ± 0.6[d]

[a] Calculated value from the equation by Pace et al. (*45*). [b] Co(III) titration (*19*). [c] Cu(II) titration. [d] From He et al. (*19*).

exponential functions, giving R^2 values (coefficients of determination) greater than 0.99 in every case.

EPR Spectroscopy. Frozen solution EPR spectra of copper and iron transferrins were obtained at 90 K with a laboratory constructed X-band (9.4 GHz) EPR spectrometer described elsewhere (*31*) using a flow of cold N_2 gas with an Air Products Helitran cryostat. *g*-Factors and hyperfine splittings were measured with the standard and unknown samples in separate halves of a TE_{104} dual cavity. Standards employed were Varian strong pitch ($g = 2.0028$) and Mn^{2+} in CaO (span of the $\pm^1/_2$ $\pm^3/_2$ and $\pm^5/_2$ lines = 86.29, 258.80, and 431.38 ± 0.04 G, respectively, $g = 2.0011$) blended with a single line coal sample ($g = 2.0035$) in an EPR tube under vacuum. Frequencies were measured with a Hewlett-Packard 5350A microwave frequency counter. Typical spectrometer settings for iron and copper samples, respectively, were microwave frequency = 9.386 and 9.380 GHz; microwave power = 20 and 10 mW; modulation amplitude = 10 and 1.0 G; scan rate = 4 and 1.2 G/s; and time constant = 1.0 and 0.3 s, respectively. Q-band (34.7 GHz) ^{63}Cu EPR spectra were measured at 104 K at a microwave power of 1.5 mW and a 100 KHz field modulation of 3.2 G using a Varian E-9 spectrometer/E-110 Q-band microwave bridge and a TE_{011} ribbon-wound cylindrical cavity (*32*). Frequency/field ratios were calibrated to five significant figures using standard samples. *g*-Factors measured from both X-band and Q-band spectra of the same sample were in excellent agreement. Powder spectra simulations were carried out with the software program SimFonia (a gift of Bruker Instruments).

RESULTS

Iron Binding: (*a) Electronic Spectra*. The absorption spectra in the visible region showing the characteristic λ_{max} (*23*, *26*) for each mutant, together with that for wild-type hTF/2N, are given in Figure 2. The spectrum of mutant Y96F is very similar to that of the wild-type protein, showing that mutation of this nonbinding ligand has no effect on iron binding. The absorption band for mutant Y95F has a considerable blue shift, with the λ_{max} at 410 nm compared to 472 nm for wild-type hTF/2N, suggesting an increased Tyr188(O)−Fe interaction in Y95F. Interestingly, there is no absorption band in the spectrum of mutant Y188F. The spectrum is similar to that for apo-hTF/2N, indicating that no iron binding occurs in mutant Y188F.

To verify that Y188F does not bind iron under normal conditions, difference spectra were taken for the apo-protein loaded with 90% of an equivalent amount of Fe(II)-nitrate in HEPES (50 mM) solution containing bicarbonate (15 mM) at pH 7.4. Figure 3A shows the difference spectra for the proteins including wild-type. Again, the Y96F mutant and wild-type hTF/2N are similar, showing maxima at 295 and 472 nm. In the case of the Y95F mutant, a shoulder at 295 nm can be distinguished in addition to the absorption band at 420 nm. In contrast, mutant Y188F shows no absorption band in either the ultraviolet or the visible region. The

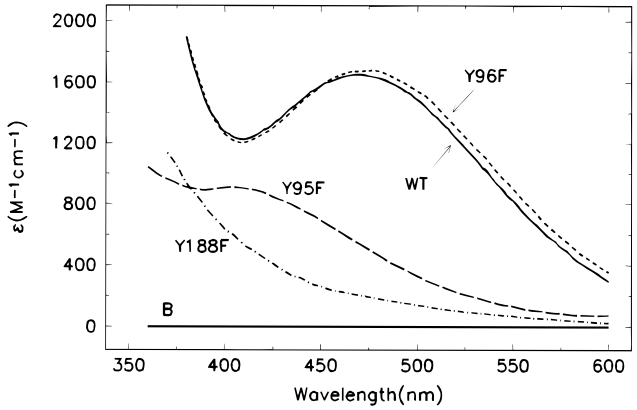

FIGURE 2: Visible spectra for the iron saturated complexes of hTF/2N with carbonate. Concentrations were calculated with the ϵ_{280}s listed in Table 1. HEPES (20 mM), pH 7.4. (B) Baseline; (WT) Wild-type hTF/2N.

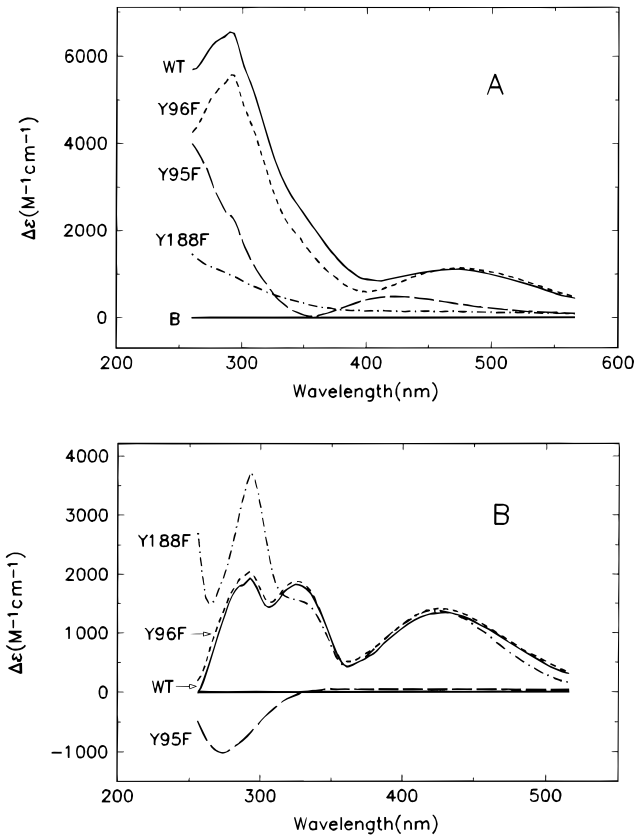

FIGURE 3: Difference spectra for metal binding (90% saturation) to hTF/2N proteins with carbonate at pH 7.4, B for baseline and WT for wild type. Concentrations were calculated with the ϵ_{280}s listed in Table 1. (A) Iron binding, HEPES (50 mM), $NaHCO_3$ (15 mM); (B) Copper binding, HEPES (25 mM), $NaHCO_3$ (1 mM).

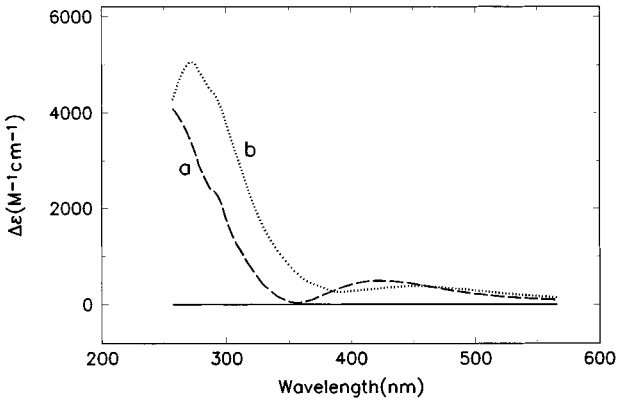

FIGURE 4: Difference spectra for the conversion from the Fe-Y95F−CO_3 to the Fe-Y95F−NTA complex. HEPES (50 mM), $NaHCO_3$ (15 mM), pH 7.4. (a) Iron saturated (90%) Fe-Y95F−CO_3 complex; (b) 1 equiv of NTA was added to the solution.

positive featureless absorbance tailing into the UV region may reflect nonspecific iron binding; a faint yellow color is observed in a concentrated solution containing this mutant and ferric ion.

Some of the intrinsic spectral parameters, λ_{max}, λ_{min}, A_{max}/A_{min}, A_{280}/A_{max} (*23*), obtained from the normal spectra, are listed in Table 1. Since the Y188F mutant cannot form the natural ferric complex with carbonate, there are no data for Fe-Y188F−CO_3. Attempts to obtain these parameters for Fe-Y188F−NTA failed (see below). The A_{280}/A_{max} value for the Y95F mutant is 44.4, nearly double that found for the wild-type and the Y96F proteins, suggesting that the ferric ion interacts with the single remaining Tyr 188 ligand.

(*b) NTA Preference*. The Y95F mutant prefers NTA over carbonate in the formation of the ferric complex, since presumably one more ligand donor group is needed to reach the favored six-coordination of iron. Difference UV−vis spectra (Figure 4) show that, when 1 equiv of NTA is added to the Fe-Y95F−CO_3 solution, the absorption band at 420 nm shifts to 455 nm, and a peak at 272 nm develops. Both peaks at 272 and 455 nm are evidence for strong NTA ligation with Fe-Y95F, which occurs in the presence of an approximately 500-fold excess of bicarbonate.

In the presence of NTA, mutant Y188F also shows iron binding. Difference spectra for the titration of the apo-Y188F with Fe(III)-$(NTA)_2$ at pH 7.4 displayed peaks at 312 and 472 nm, respectively, indicating binding at the specific iron-binding site (Figure 5A). However, the complex is weak. Figure 5B shows the titration data taken at A_{312} and A_{472}. Fitting these data with a saturation function (Hill), $A = S_{max}R/(k + R)$, where S_{max} is the absorbance for saturation binding, R is the molar ratio of iron to protein, and k is a constant, revealed that at least a 32-fold excess of $Fe(NTA)_2$ was needed to reach 95% saturation. Futhermore, such weakly bound iron can be reversed with HEPES buffer (pH 7.4, four changes), resulting in the spectrum of the apoprotein.

(*c) EPR Spectra*. Iron EPR spectra (Figure 6) for the three tyrosine mutants and wild-type hTF/2N confirmed the results derived from the electronic spectra. These spectra were taken for the iron-loaded samples with 90% metal saturation in HEPES buffer (pH 7.5) in the absence of NTA. The Fe-Y96F protein has a typical spectrum of transferrin, equivalent to that for the wild-type protein, showing three features near $g' = 4.3$ (*24*). In contrast, pronounced changes were

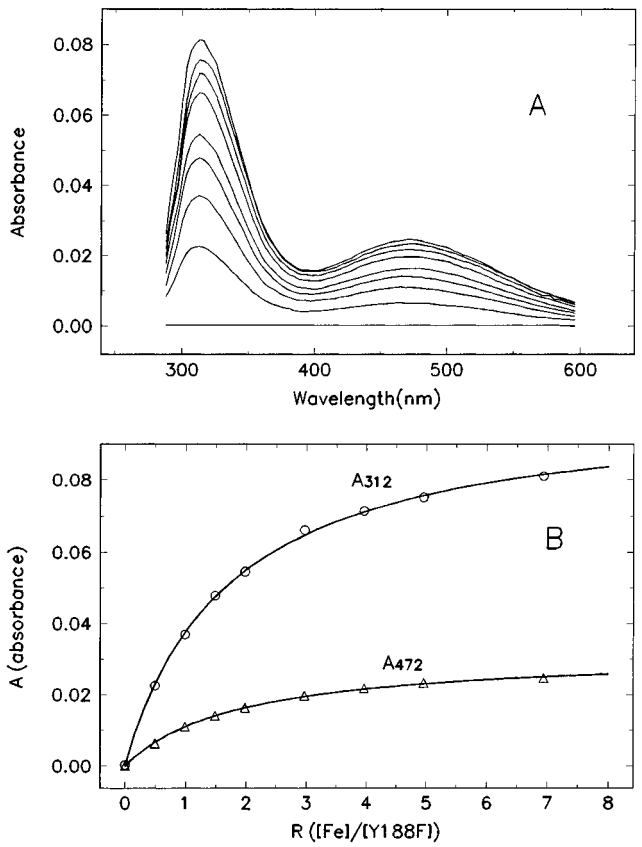

FIGURE 5: Spectral data for the titration of $Fe(NTA)_2$ to the apo-Y188F mutant. HEPES (25 mM), pH 7.4. (A) Difference spectral absorption after adding a given amount of $Fe(NTA)_2$ and equilibration. (B) Absorbance data at different concentration ratios of [Fe]/[Y188F] and the curves fit with a saturation function $A = S_{max}R/(k + R)$.

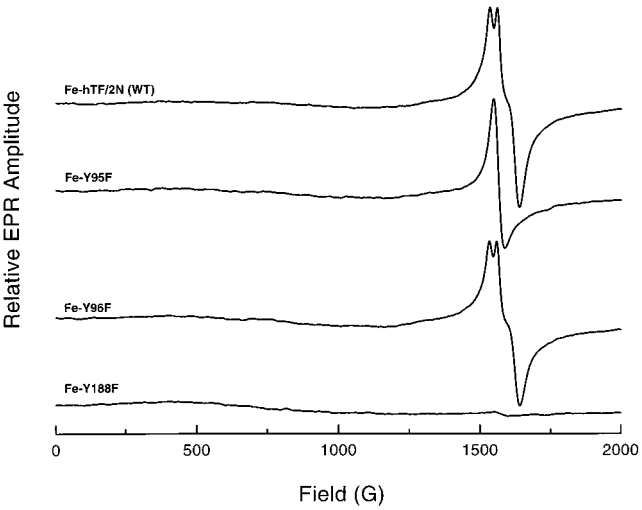

FIGURE 6: X-band (9.38 GHz) EPR spectra of frozen samples of 90% iron saturated hTF/2N and various tyrosine mutants. Protein samples (∼0.3 mM), HEPES (∼0.1 M), and $NaHCO_3$ (∼10 mM), pH 7.5, temperature 90 K. See Materials and Methods for instrument settings.

observed in the spectrum for the Y95F mutant, showing pure rhombic spectral features. The spectral change from slightly axial in Fe-hTF/2N to purely rhombic in mutant Y95F suggests a significant difference in iron coordination between the two. The EPR spectrum of Y188F showed no signal (Figure 6), confirming again that no iron binds to this mutant under the conditions used with the other samples.

Table 2: Rate constant k (min^{-1}) for Metal Release from the Proteins[a]

protein	Fe removal[b] [KCl] = 0	Fe removal[b] [KCl] = 0.14 M	Cu removal[c] [KCl] = 0
Y95F	1.65[d]		
Y96F	0.027	0.015	5.54
Y188F			0.023
WT	0.022	0.018	4.25

[a] HEPES buffer (50 mM, no $NaHCO_3$), pH 7.4, 25 °C. [b] Iron removal by Tiron (12 mM) except for the Y95F. [c] Copper removal by EDTA (8 mM). [d] Iron removal by EDDA (0.8 mM).

(*d) Iron Release*. Iron release kinetics were carried out to determine quantitatively the relative lability of each protein. The results are listed in Table 2. Under identical conditions, iron release from both the Y96F and wild-type hTF/2N by Tiron is similarly slow, both in the presence and absence of KCl. As might be expected, iron release from the Fe-Y95F is very facile. Even when the comparatively weak chelator EDDA (log K = 16.9 and 26.5) (*33*) instead of Tiron (log K = 20.2, 35.3, and 45.5) (*33*) is used, iron release from the ferric Y95F is fast, being complete within 10 min.

Copper Binding: (a) Electronic Spectra. The inequivalence of the two tyrosine ligands in hTF/2N is also evident in the binding of copper(II). Of interest, however, is the fact that mutant Y188F binds copper tightly, whereas mutant Y95F does not bind copper at all. Figure 3B shows the difference spectra for the copper binding of the mutants and wild-type hTF/2N with 90% copper(II) saturation at pH 7.4. Both the wild-type hTF/2N and mutant Y96F show similar copper binding. Mutant Y188F demonstrates its preference for copper binding with intense absorptions both in UV and visible regions. In contrast, the spectrum of mutant Y95F shows no absorption bands indicative of copper binding; the broad negative absorption may signify the binding of the anion to the apo-protein (*34*).

Copper binding to transferrins results in a bright yellow color. In the case of mutant Y188F, the reaction with copper is completed instantly, allowing determination of the absorption coefficient for this mutant. The resulting ϵ_{280} value, together with that for mutant Y96F derived from Co(III) titration (*19*) and the common spectral characteristics for the copper complexes, is given in Table 1.

(b) EPR Spectra. X-band ^{63}Cu EPR spectra Cu_2-hTF, Cu-hTF/2N, Cu-Y95F, Cu-Y96F, and Cu-Y188F are shown in Figure 7. To enhance the resolution of fine structure, spectra were obtained in D_2O with a field modulation of only 1 G. The triplet fine structure on the low field parallel line shown on expanded scale in Figure 7 arises from the ^{14}N nucleus of the histidine in the specific metal-binding sites of the protein (*35*−*37*). Parallel EPR spin Hamiltonian parameters were obtained from simulation of the line positions to second-order using the program SimFonia. Attempts to obtain perpendicular parameters from simulation of the perpendicular region of the X-band spectra of the various proteins using values similar to the spin Hamiltonian parameters reported in the literature (*35*, *37*, *38*) were unsuccessful. Consequently, values of g_x and g_y were obtained from Q-band spectra (Figure 8). These spectra lack fine structure due to g-strain broadening of the EPR lines at higher field. The EPR parameters from analysis of the X- and Q-band spectra

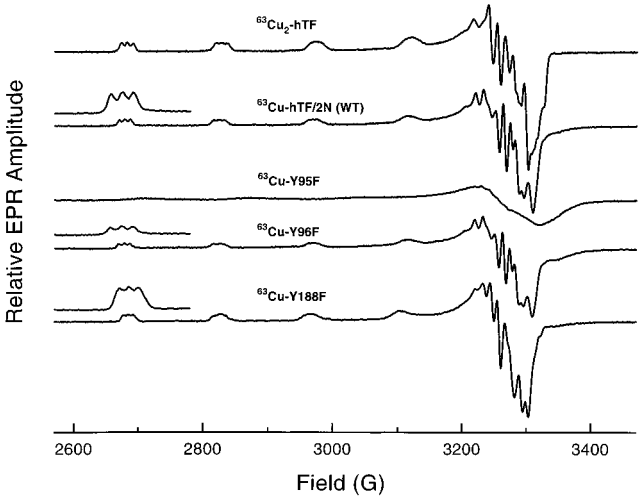

FIGURE 7: X-band (9.38 GHz) EPR spectra of frozen samples of 90% ^{63}Cu saturated hTF, hTF/2N, and various tyrosine mutants. Protein samples (∼0.5 mM), HEPES (∼0.1 M), $NaHCO_3$ (∼20 mM), in D_2O, pD 7.9. Temperature 90 K. See Materials and Methods for instrument settings. The triplet features are expanded 2-fold in magnetic field.

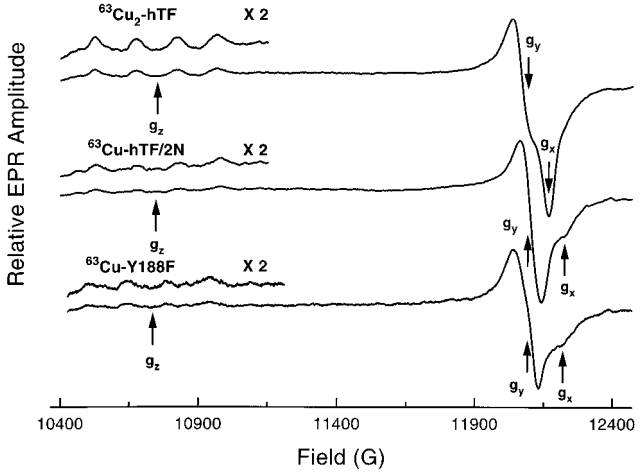

FIGURE 8: Q-band (34.7 GHz) EPR spectra of frozen samples of $^{63}Cu_2$-hTF, ^{63}Cu-hTF/2N and ^{63}Cu-Y188F at 103 K. The samples are the same as in Figure 7. See Materials and Methods for instrument settings.

are summarized in Table 3 along with literature values for Cu_2-hTF. For comparison with literature values, ^{63}Cu hyperfine splittings measured here have been scaled to ^{65}Cu values using the relative magnitudes of the nuclear moments of the two isotopes.

The ^{63}Cu EPR spectra show clear evidence for differences in copper binding by Cu_2-hTF, Cu-hTF/2N and the various tyrosine mutants. All of the spectra show fine structure with the exception of mutant Y95F where the EPR spectrum is similar to that found with buffer alone. This result confirms that mutation of ligand Tyr 95 results in a protein which is unable to bind copper specifically. In contrast, mutation of the ligand Tyr 188 results in a protein capable of binding copper but which displays an altered fine structure spectrum (Figure 7 and Table 3). In the case of wild-type Cu-hTF/2N and Cu-Y96F, the spectra are identical (Figure 7), in accord with the UV−visible spectral and copper removal data (Figure 2, Tables 1 and 2).

(*c) Copper Removal*. While EPR and UV−vis spectra indicate that copper binding occurs, the kinetics of copper

Table 3: ^{65}Cu EPR Parameters[a]

protein	g_x	g_y	g_z	a_x^{Cu}	a_y^{Cu}	a_z^{Cu}	a_x^N	a_y^N	a_z^N
Cu_2-hTF[b]	2.043 (2.042)	2.060 (2.059)	2.312 (2.312)	(<30)	(<30)	155.9 (155.1)	(11.0)	(11.0)	9.2 (9.5)
Cu-hTF/2N	2.035	2.056	2.315			157.3			8.7
Cu-Y96F	2.035	2.056	2.315			157.3			8.7
Cu-Y188F	2.037	2.056	2.319			150.9			7.8

[a] Hyperfine splittings in units of Gauss. Measured ^{63}Cu hyperfine splittings have been converted to ^{65}Cu values using the relationship $a(^{65}Cu) = a(^{63}Cu)g_n(^{65}Cu)/g_n(^{63}Cu)$ where the nuclear g-factors are $g_n(^{65}Cu) = 1.588$ and $g_n(^{63}Cu) = 1.484$. Errors in g are nominally ± 0.001, in a^{Cu} nominally $\pm$ 0.5 G and in a^N nominally ± 0.2 G. [b] Literature values are given in parentheses (*35*, *37*).

removal can be used to estimate the relative labilities of the complexes. The first-order kinetic constants, acquired by means of our established spectrophotometric procedure, are given in Table 2 (*26*). Under identical conditions, Cu-Y96F has a slightly faster rate of copper release to EDTA than Cu-hTF/2N(WT), whereas copper removal from Cu-Y188F mutant is about 200 times slower than that from the wild-type protein. Only a few minutes is required to remove copper completely from the wild-type protein compared to approximately 2 h for 90% copper removal from Cu-Y188F, consistent with a much tighter copper binding in Y188F.

DISCUSSION

Iron Binding and Release. Metal binding to transferrin produces two ultraviolet absorption peaks near 242 and 295 nm, which can be observed in the difference spectrum between the metalloprotein and the apo-protein. These absorptions are attributed to metal complexation with the tyrosine ligands that perturbs the π to π^* transitions of the aromatic ring (*39*). When the metal ions have unpaired d electrons, the binding with transferrin results in another intense visible absorption in 410−500 nm range, which is assigned to the charge transfer between phenolate (π) and the metal ions (dπ^*) (*39*, *40*). These spectral absorptions, especially those in the visible region, are the absorption bands for metal-binding, and are used as an indicator of specific metal-tyrosine binding in transferrin.

Both normal and difference UV−vis spectra and EPR spectra for iron binding with the proteins revealed that the Y96F mutant has an analogous iron binding to the parent hTF/2N. This is reasonably accounted for by the absence of tyrosine 96 side-chain coordination to iron in the protein. Unexpectedly, the two mutants Y95F and Y188F show very different iron-binding behavior. Under identical conditions, the Y95F mutant binds iron but the Y188F protein does not, displaying an interesting inequivalence of these two ligands in the function of the protein. Tyr 95 comes from a hinge strand whereas Tyr 188 resides in an α-helix and is the only ligand from domain II (*6*). In the distorted octahedral structure of iron coordination, Tyr 95 occupies an equatorial position, whereas Tyr 188 binds to the iron center at an apical position with a longer Fe-O(Tyr) bond (*16*). The loss of the Tyr 95 ligand does not destroy coordination since the binding to iron is still able to bring the two domains together to close the cleft by linking the ligand Asp 63 on domain I and the ligand Tyr 188 on domain II. The coordination site of the missing Tyr 95 ligand may possibly be occupied by a water molecule in the mutant. The weaker ligation of the water may allow a stronger Fe-O(Tyr 188) interaction, resulting in a large observed blue shift in the λ_{max} from 472 to 410 nm in mutant Y95F. The rhombic EPR spectral feature of Fe-Y95F (Figure 6) also reveals a different iron binding motif for the mutant. Correspondingly, mutant Y95F shows a preference for NTA as the synergistic anion. NTA with its three potential ligand donors replaces carbonate even in a solution containing more than 500-fold excess bicarbonate, perhaps to satisfy the six-coordinate requirement of the iron upon loss of a protein ligand. The formation of the stable complex, Fe-Y95F−NTA, suggests there is inner flexibility in the cleft.

Both UV−vis and iron EPR spectra clearly show that mutant Y188F does not bind iron specifically with carbonate as the synergistic anion. It seems reasonable to speculate that the loss of the only ligand on domain II leads to a failure of cleft closure. Even when full six coordination was provided to the ferric iron by joining with NTA, the resulting complex was still relatively labile (see Results), indicating, perhaps, the absence of a closed conformation. This situation appears to differ from that in the D63 mutants of hTF/2N (*26*). The loose conformation caused by mutation in the D63 mutants may make the iron binding weak and iron removal facile (*26*), but an "open" conformation resulting from the loss of the Y188 ligand leads to the complete absence of a stable iron complex.

Tyrosine 188, the Most Critical Ligand for Iron Binding. Of the four iron-binding ligands from the protein, the histidine and aspartate are the two for which the importance in the coordination structure and properties of metal binding to transferrin has been investigated in detail. A comprehensive study of the liganding histidine (His 253) in hLF N-lobe has been reported recently (*22*). When this histidine was mutated to 11 different residues, in all cases the iron-binding affinity of the protein was impaired but not abolished, irrespective of whether the substituted amino acids were potential iron ligands or not. The iron-binding behaviors of the histidine variants of hTF/2N, H249Y (*25*), H249E, and H249Q (*24*) also have been studied. Compared to the parent hTF/2N, the H249Y mutant shows a faster iron release rate (*25*) and the H249E and H249Q mutants display significantly different EPR spectra, reflecting a diverse iron coordination (*24*).

Mutations at the aspartate ligand also destabilized the structure and the iron binding of transferrins (*21*, *23*, *26*). The aspartate ligand appears to play a particularly important role in both iron binding and cleft closure (*21*). Several aspartate mutants, D60S of hLF N-lobe (*21*) and D63A, D63C, D63E, D63N, and D63S of hTF/2N (*23*, *26*), have been made to address the influence of mutations on metal binding. In all cases, iron-binding stability of the proteins was significantly impaired. However, even for D63A, the iron-binding capacity was not destroyed completely, although the substituted Ala 63 lacks any possibility for iron binding and hydrogen bonding leading to interdomain contacts.

There are a limited number of reports concerning the effect of the tyrosine ligands on the iron binding of the protein. Zak et al. observed that when the Tyr 95 ligand in hTF/2N was mutated to histidine, the iron release behavior of the resulting mutant, Y95H, did not show any apparent difference from that of the wild type N-lobe (*25*). On the other hand, when the two tyrosine ligands in either lobe of lactoferrin were changed simultaneously to alanine, the lobe lost iron-binding ability completely, as would be expected (*27*). In the present report, detailed studies have been performed to address the importance of the tyrosine ligands. As described above, mutant Y95F is still able to bind iron although the binding is weak, but the Y188F mutant entirely fails to form a natural Fe-Y188F-CO_3 complex. This is the only single-point mutation to date in which the natural iron binding is completely abolished.

Copper Binding and Removal. Copper binding of transferrins is weak [log K_1 for Cu-ovotransferrin is ~12 (*20*), compared to ~20 for ferric transferrin (*42*)] but stable. A characteristic absorbance at ~425 nm for copper binding with transferrin can be employed to monitor the specific binding and forms the basis of spectrophotometric studies. With its d^9 electron configuration, copper(II) gives rise to typical and much-used EPR signals that provide useful information about transferrin structure. A high-resolution study of copper(II)-substituted lactoferrin has recently been reported and it is the only metal complex, other than iron-loaded transferrin, for which crystallographic data are available (*18*). In the N-lobe of hLF, the copper is five coordinate, square pyramidal, with a long apical bond to one tyrosine ligand (Tyr 92) and a monodentate carbonate anion, Asp 60, His 253 and Tyr 192, in that order, comprising the equatorial plane. In the present study the wild-type hTF/2N is assumed to have a similar copper binding mode with the hLF N-lobe although as indicated below this assumption may not be correct.

Since the Tyr 96 side chain in hTF/2N is not a ligand, and does not take part in any other ligation around the metal center, Cu-Y96F exhibits electronic and EPR spectra essentially identical to the wild-type protein (Figures 3B and 7, Tables 1 and 3) and has a similar copper removal rate (Table 2). The ^{14}N superhyperfine splitting ($a_z^N = 8.7$ G) comes from coupling with the unpaired electron residing in the d_{x2-y2} orbital of the Cu^{2+} ion. Thus, His 249 must be in the equatorial plane of the copper in Cu-hTF/2N, a result consistent with the X-ray structure of the N-lobe of dicupric lactoferrin (*18*). The direction of g_z (=2.315) is therefore expected to be approximately along the Cu-Tyr(95) apical bond. In this connection, the failure of mutant Y95F to bind Cu^{2+} (Figures 3B and 7) is somewhat surprising given the apical position of this ligand, its rather long bond length (2.8 Å) in the corresponding copper lactoferrin structure (*18*) and the fact that it is not required for Fe^{3+} binding. Protein conformation, in addition to the first-coordination sphere of the Cu^{2+} ion, evidently plays an important role in determining the overall stability of the complex.

In contrast, mutant Y188F binds copper relatively tightly, but with altered UV−visible and EPR spectra relative to the wild-type protein (Figures 3B, 7, and 8). The spin Hamiltonian parameters reveal a significant change in copper coordination with this mutation, most notably the reduction in a_z^{Cu} from 157.3 G in Cu-hTF/2N to 150.9 G in Cu-Y188F and a_z^N from 8.7 to 7.8 G (Table 3). The reduction in a_z^N in Cu-Y188F indicates a diminished interaction with His 249 for this mutant, possibly reflecting an increase in the Cu-N bond length. Loss of Tyr 188 in the equatorial plane of the copper may result in considerable reorganization of the metal binding site, accounting for the large reduction in a_z^{Cu} and changes in the perpendicular region of the spectrum (Figure 7).

The equivalence of the binding sites of transferrin when occupied by copper has been a matter of long standing interest. Reported line broadening and increased line asymmetry in S-band and X-band EPR spectra of dicupric *vs* monocupric transferrin complexes suggest a slight inequivalence between the two metal-binding sites (*36*, *38*, *41*) whereas higher resolution ^{14}N, ^{65}Cu, and ^{1}H ENDOR measurements are consistent with the two sites being equivalent within resolution of the ENDOR lines (*37*). Significantly, the EPR spectrum of Cu-hTF/2N reported here is quite different from that of dicupric transferrin at both X- and Q-band, particularly in the perpendicular region of the spectrum (Figures 7 and 8). Thus, the data suggest that the presence of the C-lobe influences the spectral properties of the N-lobe. Furthermore, the *g*-strain broadening of the parallel lines in the Q-band EPR spectra of Cu-hTF/2N is greater than that of Cu_2-hTF (Figure 8), making these lines more difficult to observe in the former and suggesting greater conformational flexibility in the half molecule than in the bilobal protein. Other studies have suggested cooperativity between the two lobes of transferrin in iron binding and release, consistent with the spectral observations reported here (*42*−*44*).

In Y188F the NII domain is presumed to be flexible since it lacks contact with the metal center via Tyr 188. However, the copper removal kinetics are unexpectedly slow (Table 2), suggesting that despite the lack of a tightly closed conformation of the NI and NII domains, mutant Y188F has a favorable environment for copper binding. The inequivalence of the two tyrosine ligands in iron and copper binding of transferrins is opposite, implying that, apart from conformational factors, the preferred coordination geometry and charge of the metal ion plays an important role in metal binding to transferrin. Efforts to crystallize the Cu-Y188F mutant are under way to determine the structural details which may account for the differences which are found.

In summary, strong evidence described here reveals that the two tyrosine ligands are not equivalent; they both play a crucial but different role in the metal binding properties of the protein. More importantly, the tyrosine 188 ligand is critical for normal iron binding; without it, the iron binding ability of the protein is totally eliminated.

ACKNOWLEDGMENT

The authors thank Mr. Junlong Shao of the University of New Hampshire for measuring the Q-band EPR spectra.

REFERENCES

1. Harris, D. C. and Aisen, P. (1989) in *Iron Carriers and Iron Proteins* (Loehr, T. M., Ed.) pp 239−351, VCH Publishers, Inc, New York.
2. Chasteen, N. D. and Woodworth, R. C. (1990) in *Iron Transport and Storage* (Ponka, P., Schulman, H. M., and Woodworth, R. C., Eds.) pp 68−79, CRC Press, Boca Raton, FL.

3. Griffiths, E. (1987) in *Iron and Infection* (Bullen, J. J. and Griffiths, E., Eds.) pp 1−25, John Wiley & Sons, Chichester.
4. Anderson, B. F., Baker, H. M., Norris, G. E., Rumball, S. V., and Baker, E. N. (1990) *Nature 344*, 784−787.
5. Anderson, B. F., Baker, H. M., Dodson, E. J., Norris, G. E., Rumball, S. V., Waters, J. M., and Baker, E. N. (1987) *Proc. Natl. Acad. Sci. U.S.A. 84*, 1769−1773.
6. Zuccola, H. J. (1993) *The crystal structure of monoferric human serum transferrin*. Thesis, Georgia Institute of Technology, Atlanta, GA.
7. Bailey, S., Evans, R. W., Garratt, R. C., Gorinsky, B., Hasnain, S. S., Horsburgh, C., Jhoti, H., Lindley, P. F., Mydin, A., Sarra, R., and Watson, J. L. (1988) *Biochemistry 27*, 5804−5812.
8. Kurokawa, H., Mikami, B., and Hirose, M. (1995) *J. Mol. Biol. 254*, 196−207.
9. Pecoraro, V. L., Harris, W. R., Carrano, C. J., and Raymond, K. N. (1981) *Biochemistry 20*, 7033−7039.
10. Harris, W. R. (1986) *J. Inorg. Biochem. 27*, 41−52.
11. Harris, W. R. (1989) *Adv. Exp. Med. Biol. 249*, 67−93.
12. Harris, W. R. (1983) *Biochemistry 22*, 3920−3926.
13. Zak, O., and Aisen, P. (1988) *Biochemistry 27*, 1075−1080.
14. Abdollahi, S., Harris, W. R., and Riehl, J. P. (1996) *J. Phys. Chem. 100*, 1950−1956.
15. Schlabach, M. R., and Bates, G. W. (1975) *J. Biol. Chem. 250*, 2182−2188.
16. Baker, E. N. (1994) *Adv. Inorg. Chem. 41*, 389−463.
17. Harris, W. R., and Madsen, L. J. (1988) *Biochemistry 27*, 284−288.
18. Smith, C. A., Anderson, B. F., Baker, H. M., and Baker, E. N. (1992) *Biochemistry 31*, 4527−4533.
19. He, Q.-Y., Mason, A. B., and Woodworth, R. C. (1996) *Biochem. J. 318*, 145−148.
20. Hirose, J., Fujiwara, H., Magarifuchi, T., Iguti, Y., Iwamoto, H., Kominami, S., and Hiromi, K. (1996) *Biochim. Biophys. Acta 1296*, 103−111.
21. Faber, H. R., Bland, T., Day, C. L., Norris, G. E., Tweedie, J. W., and Baker, E. N. (1996) *J. Mol. Biol. 256*, 352−363.
22. Nicholson, H., Anderson, B. F., Bland, T., Shewry, S. C., Tweedie, J. W., and Baker, E. N. (1997) *Biochemistry 36*, 341−346.
23. Woodworth, R. C., Mason, A. B., Funk, W. D., and MacGillivray, R. T. A. (1991) *Biochemistry 30*, 10824−10829.
24. Grady, J. K., Mason, A. B., Woodworth, R. C., and Chasteen, N. D. (1995) *Biochem. J. 309*, 403−410.
25. Zak, O., Aisen, P., Crawley, J. B., Joannou, C. L., Patel, K. J., Rafiq, M., and Evans, R. W. (1995) *Biochemistry 34*, 14428−14434.
26. He, Q.-Y., Mason, A. B., Woodworth, R. C., Tam, B. M., Wadsworth, T., and MacGillivray, R. T. A. (1997) *Biochemistry 36*, 5522−5528.
27. Ward, P. P., Zhou, X., and Conneely, O. M. (1996) *J. Biol. Chem. 271*, 12790−12794.
28. Nelson, R. M., and Long, G. L. (1989) *Anal. Biochem. 180*, 147−151.
29. Funk, W. D., MacGillivray, R. T. A., Mason, A. B., Brown, S. A., and Woodworth, R. C. (1990) *Biochemistry 29*, 1654−1660.
30. Mason, A. B., Funk, W. D., MacGillivray, R. T. A., and Woodworth, R. C. (1991) *Protein Expression Purif. 2*, 214−220.
31. Yang, X., and Chasteen, N. D. (1996) *Biophys. J. 71*, 1587−1595.
32. Wang, W., and Chasteen, N. D. (1995) *J. Magn. Reson., Ser. A 116*, 237−243.
33. Smith, R. M., & Martell, A. E. (1976) *Critical stability constants*, Vol. 3, 4, & 5, Plenum Press, New York.
34. Cheng, Y. G., Mason, A. B., and Woodworth, R. C. (1995) *Biochemistry 34*, 14879−14884.
35. Aasa, R., and Aisen, P. (1967) *J. Biol. Chem. 243*, 2399−2404.
36. Zweier, J. L., and Aisen, P. (1977) *J. Biol. Chem. 252*, 6090−6096.
37. Roberts, J. E., Brown, T. G., Hoffman, B. M., and Aisen, P. (1983) *Biochim. Biophys. Acta 747*, 49−54.
38. Froncisz, W., and Aisen, P. (1982) *Biochim. Biophys. Acta 700*, 55−58.
39. Gaber, B. P., Miskowski, V., and Spiro, T. G. (1974) *J. Am. Chem. Soc. 96*, 6868−6873.
40. Patch, M. G., and Carrano, C. J. (1981) *Inorg. Chim. Acta 56*, L71−L73.
41. Zweier, J. L. (1978) *J. Biol. Chem. 253*, 7616−7621.
42. Aisen, P., Leibman, A., and Zweier, J. (1978) *J. Biol. Chem. 253*, 1930−1937.
43. Chasteen, N. D., and Williams, J. (1981) *Biochem. J. 193*, 717−727.
44. Thompson, C. P., Grady, J. K., and Chasteen, N. D. (1986) *J. Biol. Chem. 261*, 13128−13134.
45. Pace, C. N., Vajdos, F., Fee, L., Grimsley, G., and Gray, T. (1995) *Protein Sci. 4*, 2411−2423.

BI9719556